UMYU Scientifica, Vol. 4 NO. 2, June 2025, Pp 095 – 099
https://doi.org/10.56919/usci.2542.011
ISSN: 2955 – 1145 (print); 2955 – 1153 (online)
A periodical of the Faculty of Natural and Applied Sciences, UMYU, Katsina

ORIGINAL RESEARCH ARTICLE

Thermal Neutron Flux Estimation in the Inner and Outer Irradiation Channels of NIRR-1 Leu Core

Muhammad Anas Salis[1] and Muhammad Taha Umar[1]
[1]Physics Department, Ahmadu Bello University, Zaria-Nigeria

ABSTRACT
This research work focused on the determination of the effective cross-section and thermal neutron flux of the inner (B2) and outer (B4) irradiation channels of the Nigeria Research Reactor-1 (NIRR-1). The effective cross-section for the inner (B2) and outer (B4) irradiation channels was found to be $1.85\times10^{-22}cm^2$ and $1.28\times10^{-22}cm^2$respectively. This shows that B2 has a higher effective cross section than B4 which means that B2 will have more particle collision and produce more energy than B4. The thermal neutron flux for inner (B2) and outer (B4) irradiation channels were found to be $(4.78 \pm 0.22) \times 10^{11}\ n/cm^2s$ and $(6.86 \pm 1.86) \times 10^{11}\ n/cm^2s)$ respectively. This shows that the outer (B4) channel is more thermalized than the inner (B2) irradiation channel because the more fission, the more the thermal neutron flux produce. This signifies that B4 will produce more heat and energy than B2; meanwhile, B2 absorbed and scatter more neutrons by the materials in the reactor than B4 because B2 has lower neutron flux than B4. The results can help provide information about the reactor's operation, especially in neutron activation analysis and fuel management decisions to enhance its performance, safety, and efficiency.

ARTICLE HISTORY
Received January 15, 2025
Accepted April 25, 2025
Published May 18, 2025

KEYWORDS
LEU, NIRR-1, High purity Germanium detector (HPGe), flux monitors, calibration sources.

INTRODUCTION
Thermal neutron flux refers to the number of thermal neutrons passing through a given area in a given time. It relates to the rate of nuclear reaction in a reactor, which determines how much heat and energy a reactor can produce, and the reactor's power output. The higher the thermal neutron flux, the more heat and energy the reactor can produce. The equivalent 2200m/s thermal flux (Φ_{th}) in which a monitor sample such as Au is irradiated can be calculated.

$$\Phi_{th} = \frac{R_s - F_{cd}R_{s,cd}}{g\sigma_{th}G_{th}} \quad \ldots\ldots(1.0)$$

Where R_s and $R_{s,cd}$ are the reaction rate per atom of bare and Cd-covered isotope irradiation, g is the correction for departure from 1/v cross-section behavior, G_{th} the shielding factor for thermal neutrons, σ_{th} the thermal neutron cross-section and F_{cd} the cadmium correction factor (Karandag *et al.* 2003).

Thermal neutrons have the lowest energy and are in thermal equilibrium with the surroundings. Their energies are around 0.025eV, corresponding to the thermal motion of atoms at room temperature. They are essential in maintaining nuclear fission reactions. Epithermal neutrons have energies above thermal neutrons but below the fast neutrons (0.025eV -0.1MeV. They can contribute to certain nuclear reactions. Fast neutrons have higher energies, typically above 0.1MeV. They can cause damage to materials and contribute to certain nuclear reactions (Karandag *et al.* 2003).

Nigeria Research Reactor -1 (NIRR-1) is a nuclear research reactor located at the Centre for Energy Research and Training (CERT), Ahmadu Bello University Zaria. The reactor is a miniature neutron source reactor (MNSR), a type of light water reactor designed by China's Institute of Atomic Energy. It can produce a steady thermal power of 31kw, which became critical in 2004 with high enriched uranium (HEU), and is the only research reactor currently operating in Nigeria (Anas *et al.*, 2023; Jonah *et al.*, 2006).

NIRR-1 was converted to a low-enriched uranium (LEU) core in 2018. The conversion might have brought about changes in the neutron flux parameters on which Neutron Activation Analysis (NAA) protocols were based. Since the primary function of NIRR-1 is NAA, there is a need to determine the thermal neutron flux in the irradiation channels. These necessitate the proper determination of neutron flux in the irradiation channel of the NIRR-1. The core physics parameters of the old HEU core and New LEU core are presented in Table 1.

The NIRR-1 achieved its first criticality with the LEU fuel 2018; the neutron spectrum parameters were also

Correspondence: Muhammad Anas Salis. Physics Department, Faculty of Science, Ahmadu Bello University, Zaria-Nigerie. ✉ muhammadtahaumar@gmail.com.
How to cite: Umar, M. T., & Anas, M. S. (2025). Thermal Neutron Flux Estimation in the Inner and Outer Irradiation Channels of NIRR-1 Leu Core. *UMYU Scientifica*, 4(2), 95 – 99. https://doi.org/10.56919/usci.2542.011

determined, and the NAA facilities were standardized for optimal utilization (Anas *et al.,* 2023).

NIRR-1 has been converted from HEU to LEU, which might have brought about changes in the neutron flux parameters on which protocols for NAA were based. These necessitate the proper determination of neutron flux in the irradiation channel of the NIRR-1. This study aims to determine the thermal neutron flux in the irradiation channel of the NIRR-1 LEU core.

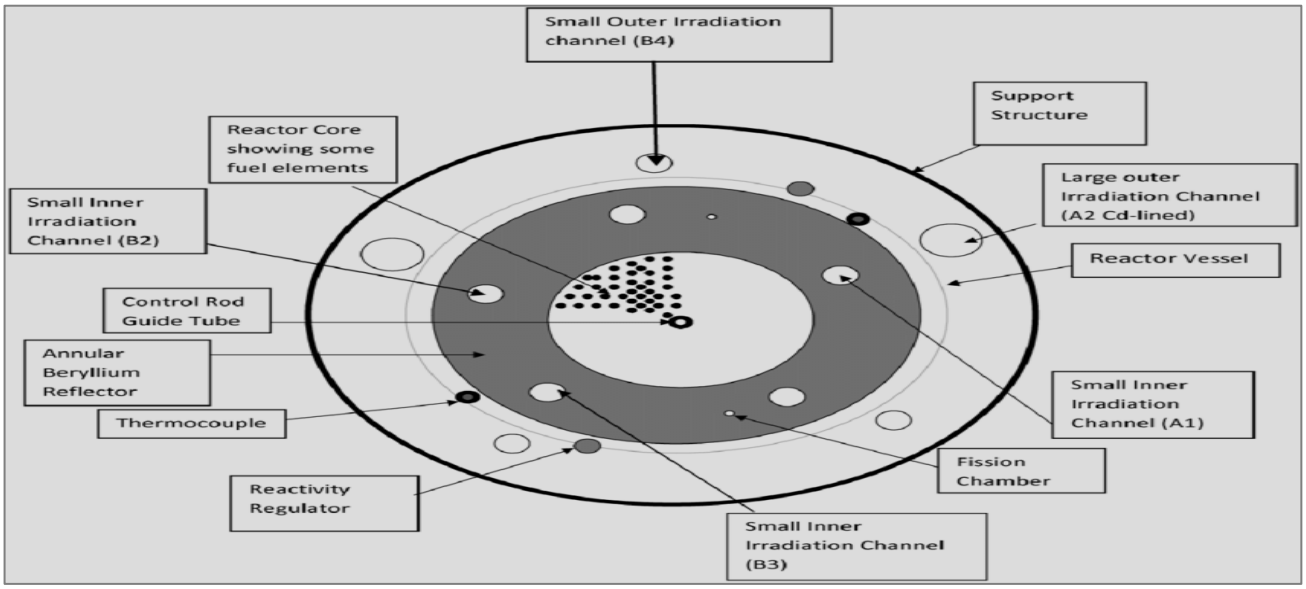

Figure 1: A layout of NIRR 1 core Configuration showing the irradiation Channels

Table 1: comparism of HEU and LEU cores of NIRR-1

Parameter	HEU	LEU
Core Diameter & Height	230 mm	230 mm
Grid Plate	Aluminium (Al)	Zircaloy-4
Number of Fuel Pins	347	335
Fuel Pin Diameter (with Cladding)	5.5 mm	5.5 mm
Fuel Length	230 mm	230 mm
Cladding Material	Aluminium	Zircaloy-4
Fuel Type	U-Al Alloy	UO_2
Enrichment of U-235	~90%	~13%
Total Mass of U-235	1.0066 kg	1.357 kg
Control Rod (CR) Diameter	3.9 mm	4.5 mm

MATERIALS AND METHODS

Materials

The materials used for this research work are NIRR-1, High purity Germanium detector (HPGe), ^{197}Au flux monitor, and calibration sources.

Methods

Cadmium-ratio (Cd-Ratio) Multi-monitor method was used to determine the neutron Spectrum Parameters. Cd-ratios of four neutron flux monitors were used to calculate the neutron flux ratio "*f*" and Epithermal flux shaping factor "α" values in the irradiation channels. The flux monitor was clean with ethanol weighed and packed in a stack inside a cleaned polyethylene capsule for the bare irradiation, while a second set was encapsulated inside a 1mm thick cadmium box for the Cd-covered irradiation channel at a thermal power level of 17kW which corresponds to preset neutron flux value of 5.0e^{11}ncm^{-2}s^{-1}. The same is done for the outer irradiation channel at the same preset neutron flux. The irradiation protocol was carried in order to induce measurable activities of at least 10,000 counts in the flux monitors (Anas *et al*., 2023).

The α and *f* values were determined iteratively using the "Solver" utility in EXCEL to solve the equations for the Au monitor.

The Neutron flux of an ideal reactor is expected to be stable during the operation. In view of this, the thermal neutron flux will be determined for the NIRR-1 new LEU core for two irradiation channels in order to establish the flux stability using Equation 2.1 (De Corte *et al*., 1981).

$$\varphi_{th} = \frac{N_p M}{w N_a \gamma \theta \varepsilon_p} \frac{1}{(1-e^{-\lambda t_i})e^{-\lambda t_d}} \frac{\lambda}{(1-e^{-\lambda t_m}) c \sigma_{eff}} \qquad (2.1)$$

where: N_p the net number of counts under the full-energy peak during counting time, t_m,

w is the weight of irradiated element,

$S = 1 - e^{-\lambda t_{irr}}$ is the saturation factor, $D = e^{-\lambda t_d}$ is the decay factor with t_d being the decay time, $C = (1 - e^{-\lambda t_m})$ is the measurement factor correcting for decay during the measurement time, t_m, M is the atomic weight, λ; is the decay constant, θ; is the isotopic abundance, N_a; is the Avogadro's number, γ; is the absolute gamma-ray emission probability,

ε_p; is the full energy peak detection efficiency, c is the concentration of the analyte and

σ_{eff}; is the effective neutron cross section in cm² as defined by (De Corte *et. al.*, 1981) and presented in Equation 3.2:

$$\sigma_{eff} = \sigma_0 \left(1 + \frac{Q_0(\alpha)}{f}\right) \quad (2.2)$$

where $Q_o(\alpha)$ is given as

$$Qo(\alpha) = \frac{Qo - 0.429}{Er^{\wedge}(\alpha)} + \frac{0.429}{(2a+1)Ecd} \quad (2.3)$$

where $Q_0 = I_0/\sigma_0$ is the ratio of resonance integral to thermal cross-section,

a is a measure of the non-ideal epithermal neutron flux distribution, and

f is the thermal to epithermal neutron flux ratio (De Corte *et. al.*, 1981).

The description of the flux monitors and their nuclear data used for the determination of Epithermal flux shaping factor "α" and flux ratio "*f*" is given in Table 2 and 3.

Table 2: Description of neutron monitoring foils used in this work.

Element	Material Description	Diameter	Range of Mass (mg)
Zn	99.95% Zn foil; 0.025 mm thick, Good Fellow	0.8 cm	8–9
Zr	99.8% Zr foil; 0.125 mm thick, Good Fellow	0.8 cm	12–14
Au	Al-0.1%Au foil; 0.1 mm thick, IRMM-530	0.8 cm	12–14

Goldman *et al., 2005*

Table 3: Nuclear data characteristics of the neutron monitoring reactions

Target Nucleus	Product Nuclide	$T_{1/2}$	Eγ (keV)	Ēr (eV)	Qo
^{68}Zn	^{69m}Zn	13.76 h	438.6	590.0	3.19
^{64}Zn	^{65}Zn	244.0 d	1115.5	2560.0	1.908
^{94}Zr	^{95}Zr	64.02 h	724.2	62600.0	5.36
^{197}Au	^{197}Au	2.695 d	411.8	5.65	15.7

The result for "α" and "*f*" were achieved by plotting a graph of Equation 3.1 as presented in Figure 2:

$$log \frac{\bar{E}_{r,i}^{-\alpha}}{(F_{Cd}.R_{Cd,i}-1)Q_{O,i}(\alpha)G_{e,i}/G_{th,i}} \text{ versus } log\, E_{r,i} \quad 3.1$$

where: $\bar{E}_{r,i}$ is the effective resonance energy of the ith monitor

F_{Cd} is the Cd-transmission factor for epithermal neutrons

$G_{e,i}$ is the epithermal neutron self-shielding factor for the ith monitor

$G_{th,i}$ is the thermal neutron self-shielding factor for the ith monitor

$R_{Cd,i}$ is the ratio of the specific activity of the ith monitor irradiated without the Cd ($A_{sp,bare}$) to that with the Cd cover ($A_{sp,\,Cd}$)

RESULTS AND DISCUSSION

Flux parameters show the nature of neutron spectrum and distribution within an irradiation channel of a research reactor. Because of this, ^{94}Zr(n,γ)^{95}Zr, ^{197}Au(n,γ)^{198}Au, ^{68}Zn(n,γ) ^{69}Zn, ^{64}Zn(n,γ)^{65}Zn and Mn^{55}(n,γ)Mn^{56} foils were used to determine the flux parameters "α" value and flux ratio "f"). All the nuclear data were adopted from De Corte 2003, as presented in (table 3). The ratio of the activity of the foil irradiated without cadmium cover to activity of the foil irradiated with cadmium cover called (Rcd) for channel B2 and B4 were presented in tables 4 and 5.

The value of the epithermal flux-shaping factor (*a*) as one of the important characteristics of each irradiation channel of a research reactor such as NIRR-1 was determined from a suitable α-monitors Au^{197}(n,γ)Au^{198}, Zr^{94}(n,γ)Zr^{95} and Zn^{64}(n,γ)Zn^{65} (table 4 to 5).

The results of the effective cross-section of the Au monitor and thermal neutron flux for the inner B2 and outer B4 irradiation channel of NIRR 1 obtained were presented in Table 6.

The effective cross-sections for inner and outer irradiation channels were 1.85×10^{-22}cm² and 1.28×10^{-22}cm², respectively. This signifies that B4 has a higher effective cross-section than B2, which means that more particles will collide and more energy will be produced in B4 than B2, which also shows the effect of effective cross-section to the rate of nuclear reaction, which is, in turn, affects the energy output of the reactor.

Table 4: showing activities irradiated foils and there Rcd at channel B2

B2-Data									
	Weight(g)			Activity (Bq)					
Monitors	Bare	Cd-cover	Energy (keV)	Bare	Cd-cover	Rcd	$Q_o(\alpha)$	logYi	LogX
Au-198	1.3E-05	1.4E-05	412.16	5804297528	2681411280	2.17	17.185	-1.2527	0.75205
Zr-97	0.04447	0.04547	756.43	272454.6397	81144.48292	3.36	340.46	0	2.52892
Zr-95	0.04447	0.04547	743.33	3360.765457	3549.825304	0.95	8.15264	-1.0864	3.79657
Mn-56	4.4E-06	4.3E-06	846.56	1029924253	57643661.68	17.87	1.32323	-1.2098	2.67025
Zn-65	0.0087	0.0083	1115.44	7185715.525	874550.7119	8.22	2.68846	-1.1106	3.40824
Zn-69	0.0087	0.0083	438.63	1.89E+12	1.40E+12	1.34	4.31139	-0.0257	2.77085

Table 5: showing activities irradiated foils and there Rcd at channel B4

B4-Data									
	Weight(g)			Activity (Bq)					
Monitors	Bare	Cd-cover	Energy (keV)	Bare	Cd-cover	Rcd	$Q_o(\alpha)$	LogYi	LogX
Au-198	1.3E-05	1.40E-05	412.16	162510244	38316395.2	4.25	16.5156	-1.7051	0.75205
Zr-97	0.04457	0.04248	756.43	198556.844	15450.4841	12.85	297.825	-1.7679	2.52892
Zr-95	0.04457	0.04248	743.33	5211.11646	4387.79466	1.19	6.7357	-1.7744	3.79657
Mn-56	4.70E-06	4.70E-06	846.56	484000027	12699934.3	38.11	1.19339	-1.6883	2.67025
Zn-65	0.0071	0.0077	1115.44	3807163.02	105171.025	36.2	2.30457	-1.8103	3.40824
Zn-69	0.0071	0.0077	438.63	16366.3035	3109.49348	5.26	3.76975	-1.496	2.77085

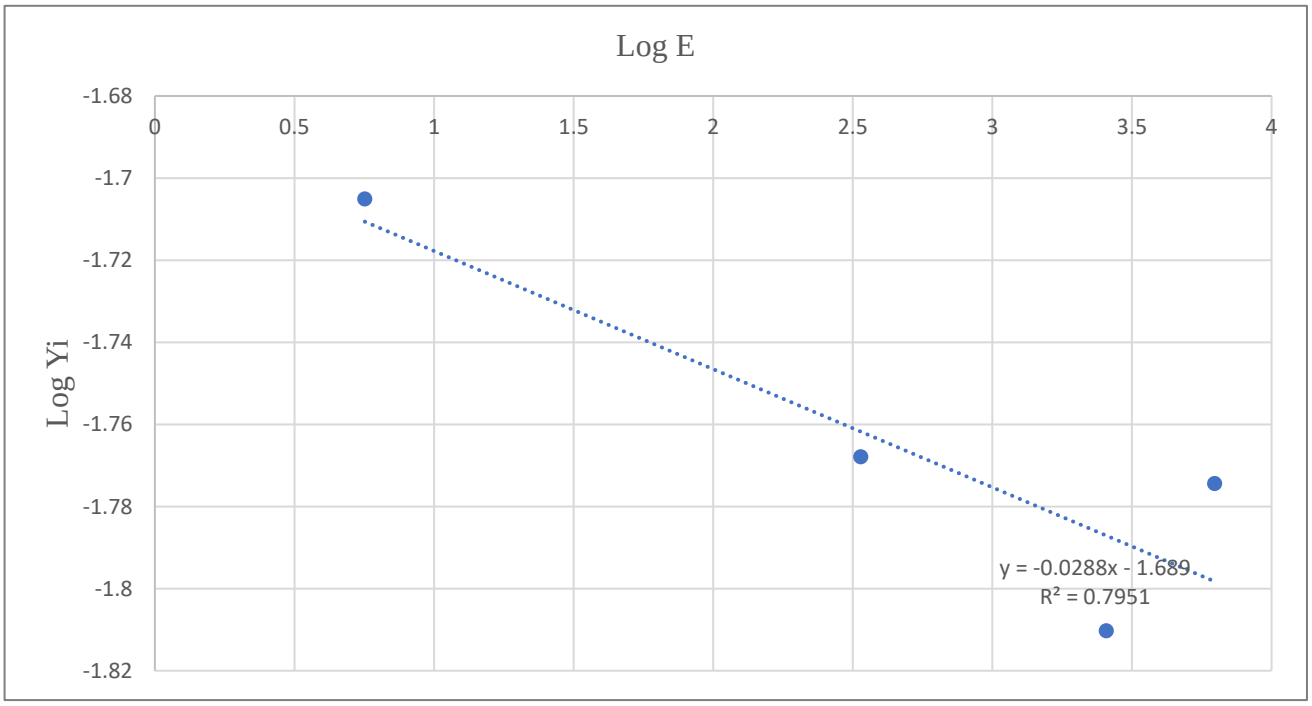

Figure 2: Cadmium ratio multi-monitor plot for (outer irradiation channel B4)

Table 6: Calculated effective cross-section of Au monitor and thermal neutron flux for inner and outer irradiation channel of NIRR 1 LEU core.

S/N	IRRADIATION CHANNELS	FOILS	σ_{eff} (x 10^{-24}cm^2)	φth (n/cm^{2}s)
1.	B2	$Au^{197}(n,\gamma)Au^{198}_{foil}$	185.1772	$4.78x10^{11}$
2.	B4	$Au^{197}(n,\gamma)Au^{198}_{foil}$	128.9955	$6.86x10^{11}$

Similarly, the thermal neutron flux, which induces fission reactions in the reactor's fuel for the inner irradiation channel (B2) and outer irradiation channel (B4) were found to be $(4.78 \pm 0.22) \times 10^{11}\ n/cm^2s$ and $(6.86 \pm 1.86) \times 10^{11}\ n/cm^2s)$ respectively. This shows that the outer (B4) channel is more thermalized

than the inner (B2) irradiation channel. This is because the more the fission the more the thermal neutron fluxes.

The effective cross-section affects the thermal neutron flux by affecting the rate at which thermal neutrons are lost in the reactor. The more neutrons that are absorbed or scattered by the materials in the reactor, the lower the neutron flux will be. This can impact the reactor's performance, including the rate of fission and the amount of energy produced. From the values obtained for the thermal neutron flux, thus, B4 is better suited for high sensitive application of NAA than B2, which signifies that B4 will produce more heat and energy than B2. Meanwhile, B2 absorbed or scattered more neutrons by the materials in the reactor than B4 because B2 has lower neutron flux than B4.

CONCLUSION

This research determined the effective cross-section of the Au monitor and the thermal neutron flux for inner (B2) and outer (B4) irradiation channels. The values obtained for the effective cross-section for inner (B2) and outer (B4) irradiation channels are $185.1772\times10^{-24}cm^2$ and $128.9955\times10^{-24}cm^2$ respectively. This shows the possibility of having more collision and energy production in the LEU core of the NIRR-1. Similarly, the thermal neutron fluxes for the inner and outer irradiation channels were found to be $(4.78 \pm 0.22) \times 10^{11}\ n/cm^2s$ and $(6.86 \pm 1.86) \times 10^{11}\ n/cm^2s)$ respectively. This shows that B4 produces more heat and energy than B2. Also B4 has more number of fission than B2.

ACKNOWLEDGEMENT

The authors are grateful to the management of CERT's entire research team, Physics Department ABU Zaria, for their support and assistance in this work.

REFERENCES

Anas, M. S., Jonah, S. A., Nasiru, R., Garba, N. N., & Muhammad, T. (2023). Development of neutron activation analysis (NAA) protocols for NIRR-1 irradiation and counting facilities after conversion to low enriched uranium (LEU) core. *Science Set Journal of Physics, 2*(1), 1–6.

Bell, G. I., & Glasstone, S. (1970). *Nuclear reactor theory*. Van Nostrand Reinhold.

De Bruin, M. (1990). Applying biological monitors and neutron activation analysis in studies of heavy-metal air pollution. *IAEA Bulletin, 32*(4), 22–27.

De Corte, F. and Simonits, A. (2003) Recommended Nuclear Data for Use in the ko Standardization of Neutron Activation Analysis. Atomic Data and Nuclear Data Tables, 85, 47-67. [Crossref]

De cortex, F., Hammami. K. S, moens, L. Simon it's, A., De wispelaere, A., Hostel, J., (1981). The accuracy of the experimental α determination in the 1/(E^1+ α) epithermal reactor neutron spectrum, journal of Radio analytical chemistry,vol 62, pp 209-255. [Crossref]

Georg, S., Stefan, M., Franziska, S., Peter, K., Christina, S., & Mario, V. (2012). Performance and comparison of gold-based neutron flux monitors. *Gold Bulletin, 45*(1), 17–22. [Crossref]

Glasstone, S., & Sesonske, A. (1994). *Nuclear reactor engineering: Reactor design basics*. Kluwer Academic Publishers. [Crossref]

Grant, C. N., Lalor, G., & Vutchkov, M. K. (1998). Neutron activation analysis of cadmium in Jamaica. *Journal of Radioanalytical and Nuclear Chemistry, 237*(1–2), 109–112. [Crossref]

Guinn, V. P. (1979). JFK assassination: Bullet analysis. *Analytical Chemistry, 51*(4), 484–493. [Crossref]

Jevremovic, T. (2009). *Nuclear principles in engineering* (2nd ed.). Springer. [Crossref]

Jonah, S. A., Umar, I. M., Oladipo, M. O. A., Balogun, G. I., & Adeyemo, D. J. (2006). Standardization of NIRR-1 irradiation and counting facilities for instrumental neutron activation analysis. *Applied Radiation and Isotopes, 64*(7), 818–822. [Crossref]

Khattab, K. (2005). Measurement of fast neutron flux in the MNSR inner irradiation site. *Applied Radiation and Isotopes, 65*(1), 46–48. [Crossref]

Levi, H. (1985). *George de Hevesy: Life and work: A biography*. A. Hilger.

Karandag, M., Yücel, H., Tan, M., & Özmen, A. (2003). Measurement of thermal neutrons and resonance integral for 71Ga(N,Γ)72Ga and 75As(N,Γ)76As by using 241Am-Be isotopic neutron source. In *Proceedings of the International Conference on Nuclear Energy* (pp. 524–527).

McLane, V., Dunford, C. L., & Rose, P. F. (2012). *Neutron cross sections*. Elsevier.

Myerscough, L. (1973). The nuclear properties of gold. *Gold Bulletin, 6*, 62–68. [Crossref]

Rutherford, E. (1920). [Archived material]. Purdue University. Archived from [original source] on 2011-08-03. Retrieved 2012-08-16.

Sanchez, I. C., Hampel, G., & Riederer, J. (2009). Reverse paintings on glass—A new approach for dating and localization. *Applied Radiation and Isotopes, 67*, 2113–2116. [Crossref]

Seabury, E. H., & Caffrey, A. J. (n.d.). *Explosives detection and identification*.